

MICROWAVE ASSISTED GREEN SYNTHESIS OF PHOTOLUMINESCENT PURE AND Mn-DOPED CADMIUM SULFIDE NANOPARTICLES

Y. KHAN, S. GUL, M. ISMAIL, M. A. KHAN, M. I. KHAN*

Department of Chemistry, Kohat University of Science & Technology, Kohat-26000 (Khyber Pakhtunkhwa) Pakistan

In this paper pure and manganese doped cadmium sulfide (CdS) nanoparticles were synthesized via a novel green route using castor oil (*Recinuscommunis*) as capping agent and hydrazine as reducing agent in deionized water. The nanoparticles were characterized by UV-visible spectroscopy, FT-IR, XRD, SEM and EDX. UV-visible spectroscopy was used to analyze optical properties of CdS. FTIR indicated presence of the various functional groups on the surface of nanoparticles. The synthesized nanoparticles were spherical in shape and poly dispersed. EDX confirmed the presence of Cd, S and Mn in the nanoparticles samples. XRD patterns gave characteristic Bragg peaks of (111), (200) and (220) which corresponded to the cubic structure of CdS nanoparticles. Intensity of photoluminescence decreased with the increase in Mn²⁺ concentration. The decrease in PL intensity of Mn-doping indicated the transfer of energy from excited carriers trapped at the surface to Mn²⁺ ions.

(Received March 27, 2017; Accepted July 24, 2017)

Keywords: Green synthesis; Microwaves; Castor oil; Mn-doped CdS; Photoluminescence property

1. Introduction

From the last few decades, nanostructured materials have been the subject of interest due to their small size, larger surface area, chemical and physical properties compared to those of bulk of the same materials. Due to small size of the nanomaterials the continuous energy band of the crystal in bulk transformed in a series of discrete states which results in widening of the effective band gap, hypsochromic shift in the optical absorption spectra, enhanced oscillator strength, size dependent luminescence and nonlinear optical effect are some of the fascinating properties revealed by these nanoparticles [1]. Semiconductor nanomaterials are of great interests for academia and industrial development owing to their distinctive size-dependent electronic and optical properties and increasing use in the fields of electrochemical cells, light-emitting diode, hydrogen producing catalyst, laser and biological labeling, photoconductive glasses for television and Xerox machines [2-4]. Among various semiconductor nanomaterials metal chalcogenide nanoparticles are particularly interesting for their use in fabrication of photodiode arrays, electrochemical cells i.e., solar cells, solar selective coatings, photoconductors, sensors etc [5]. Chalcogenides of cadmium form a technically significant class of materials due to their extensive applications in electronic and optoelectronic industries [6]. Cadmium sulfide is one of the most studied metal chalcogenide material due to its well-established relationship between the size of the particle and the optical absorption [4]. Currently, there has been growing interest in Type II-VI wide band gap semiconductor materials due to their promising physical and chemical properties and for their potential use in electronic, optoelectronic and photovoltaic devices. Cadmium sulfide is a chalcogenide n-type semiconductor nanomaterial having a wide energy band gap between 2.28-2.45 eV at room temperature [7, 8].

CdS nanoparticles have promising applications in the fields like non-linear optical devices, gas sensors, cathode ray tubes, laser and infrared microstrip detectors, various

* Corresponding author gorikhan@kust.edu.pk

luminescence devices and so on [9]. CdS nanoparticles have interesting photocatalytic degradation of dyes and better hydrogen production ability for water photolysis [10]. There is a rising interest in the use of CdS nanoparticles as luminescence probes; CdS have large amount of visible light-detecting properties among the other semiconductors. Doping is the process of mixing a precise amount of impurities to a semiconductors material which change its physical and chemical properties and electrical conductivity [11].

Various methods can be used for nanoparticles synthesis such as chemical, physical and biological synthesis; various methods reported for the synthesis of cadmium sulfide nanoparticles include chemical vapor deposition, sol-gel, spray pyrolysis, solvothermal, hydrothermal, coprecipitation, sono-chemical, microwave assisted and suspension colloidal synthesis. However, microwave assisted synthesis route offers the advantages over other methods such as short reaction time, environmentally friendly, cheap, high energy efficiency and large industrial scalable reaction [12].

As a continuation of recent efforts in the green synthesis of materials [13], in the present work, we have synthesized pure and Mn-doped cadmium sulfide nanoparticles by novel green microwave-assisted method using castor oil as capping and hydrazine as reducing agents and their structural and photoluminescence properties have been investigated.

2. Experimental

2.1. Materials

Cadmium sulphate octahydrate ($\text{CdSO}_4 \cdot 8\text{H}_2\text{O}$) and thiourea ($\text{SC}(\text{NH}_2)_2$) was purchased from BDH Laboratory Supplies (England) used as the cation and anion precursors respectively; Castor oil (*Recinus communis*) was purchased from local market used as capping agent; hydrazine hydrate a reducing agent was purchased from Daejung Korea, manganese chloride tetra hydrates ($\text{MnCl}_2 \cdot 4\text{H}_2\text{O}$) was from Daejung Korea, ethanol and deionized water used were of analytical grade.

2.2. CdS nanoparticles synthesis

For the synthesis of CdS nanoparticles, 50 mL of 0.05 M $\text{CdSO}_4 \cdot 8\text{H}_2\text{O}$ solution was taken in 500 mL volumetric flask, 1 mL of castor oil was dissolved in 20 mL of ethanol and added the solution drop wise to $\text{CdSO}_4 \cdot 8\text{H}_2\text{O}$ solution. Then added 50 mL of 0.05 M $\text{SC}(\text{NH}_2)_2$ solution, shook well and then added 50 mL of 0.05 M hydrazine hydrate solution drop wise and stirred for 5 minutes on magnetic stirrer. Then the solution was subjected to microwaves for two minutes, yellow color precipitate confirmed the formation of CdS nanoparticles. The precipitate was centrifuged at 8000 rpm for 30 minutes; supernatant liquid was discarded and the remaining solid part was dispersed in deionized water followed by washing with ethanol to remove the excess oil and other unreacted reactants. Then the precipitate was dried at room temperature and then calcined at 200 °C for 2 hours in the oven. Then 1%, 2.5%, 5% and 10% of Mn-doped CdS nanoparticles were synthesized by putting various concentrations of 0.05 mL manganese chloride tetra hydrates solution ($\text{MnCl}_2 \cdot 4\text{H}_2\text{O}$) into CdS solution by repeating the above procedure.

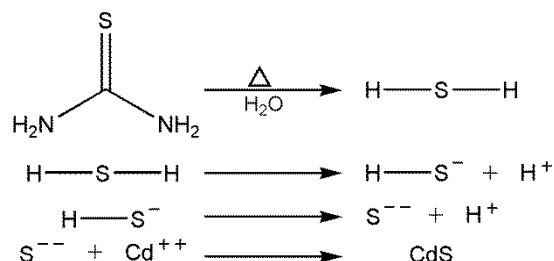
2.3. Characterization

The optical absorption spectra of CdS nanoparticles were observed using UV-visible spectrophotometer Shimadzu, UV-1800, in the wavelength range of 300 to 700 nm. Various functional groups working as capping and stabilizing agents in CdS nanoparticles were determined by SPECTRUM 100, CPU32 MAIN 00.02.7000 Fourier transformer infrared spectrometer (FTIR), in the range of 450-4000 cm^{-1} . Average crystallite size was determination using POWD-12++ by using Cu-K α radiation [$\lambda = 1.5406 \text{ \AA}$] X-ray Diffractometer. The elemental composition and surface morphology of the synthesized nanomaterials were analyzed through energy dispersive x-ray spectrometry (EDS) 6490(LA) instrument attached to the JSM-6490 scanning electron microscope (SEM). Photoluminescence (PL) spectra of the prepared nanoparticles were recorded using Model: DV 420_OE, from the range of 300 to 700 nm by software version.

3. Results and discussion

In the present green synthesis, thiourea was used as sulfide source and hydrazine hydrate as the reducing agent as well as alkaline medium source in the solution with Castor oil as capping agent. In the beginning, a light milky solution was formed and gradually became transparent when stirred, then changed from white to light yellow and finally into orange-yellow on microwave which is typical color of the cadmium sulfide formation whereas biomolecules in castor oil interacted with the CdS nanoparticles by protecting their surface.

The possible reaction mechanism of the formation of CdS nanoparticles has been summarized in the Scheme 1 below.



Scheme 1. Reaction mechanism of the formation of CdS nanoparticles

In the first step hydrogen sulfide was produced from thiourea which was further decomposed into HS^- and S^{--} , which finally reacted with the Cd^{+2} to give CdS.

3.1. UV-Visible spectra

The UV-visible absorption spectrum of pure and Mn-doped CdS nanoparticles was examined using UV-visible spectrophotometer as shown in Fig. 1. The pure CdS nanoparticles showed the absorption band at 445 nm confirming the formation of CdS nanoparticles [14]. The adsorption band for Mn doped CdS nanoparticles show hypsochromic shifted by increasing the Mn concentration i.e. 1%, 2.5%, 5% and 10% Mn-doped CdS nanoparticles have absorption bands at 341, 435, 433 and 425 nm respectively. The gradual blue shift from pure to Mn-doped CdS nanoparticles corresponded to the decrease of the size of the nanoparticles.

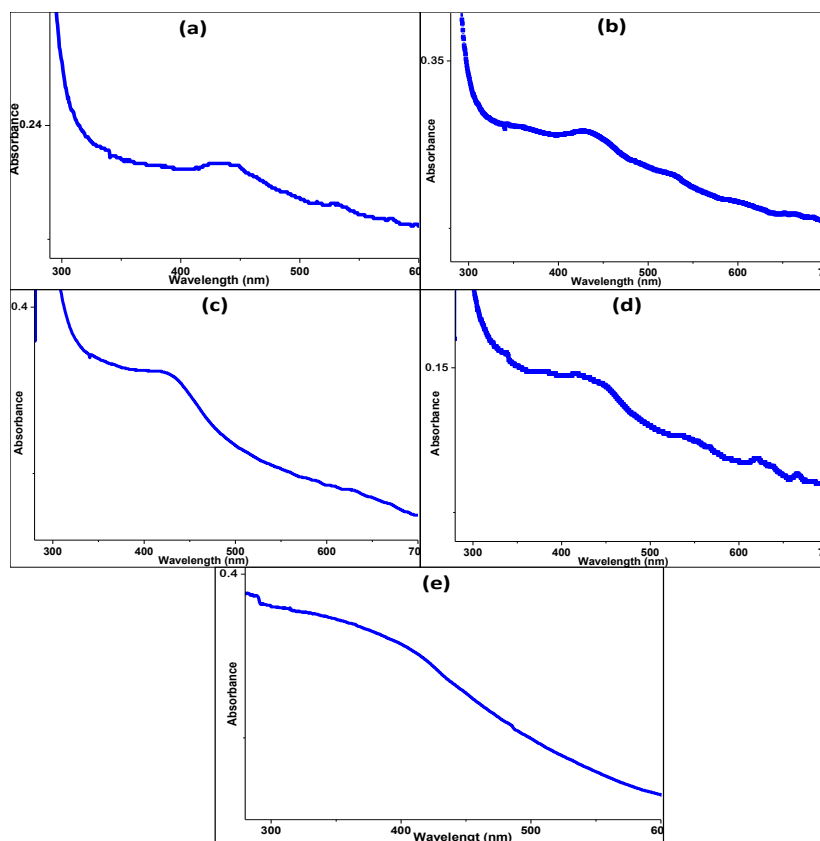


Fig. 1. UV-visible spectra of (a) pure CdS showing band at 445 nm (b) 1% Mn-doped CdS (c) 2.5 % Mn-doped CdS (d) 5% Mn-doped CdS and (e) 10% Mn-doped CdS nanoparticles

3.2. FT-IR

FT-IR spectra of the prepared nanoparticles is shown in Figure 2. A sharp band at 3425 cm^{-1} and 3360 cm^{-1} was assigned to the N-H stretching vibration. The peak at 2925 and 2854 could be attributed to the stretching vibration of asymmetric and symmetric methylene group respectively. The peak at 1749 cm^{-1} represented C=O double-bond stretching vibration of carboxylic acids. The peaks at 1635 and 1580 cm^{-1} represented the amide I and amide II peaks, respectively. The broad peaks at 1220 and 1140 cm^{-1} represented the C-N bending vibrations of aliphatic amines respectively. The band at 660 cm^{-1} confirms the formation of CdS. The observed intense peaks at 600 , 578 and 525 cm^{-1} were attributed to metal oxygen (Cd-O and C-O) stretching vibration modes [15-18]. This result indicated that there is an interaction between the carboxylic groups of -COOH and the amide groups. In FT-IR spectra no change in the peak positions of matrix was observed with doping of Mn on the CdS nanoparticles which proved that the doping of Mn on the CdS nanoparticles do not affect their chemical behavior.

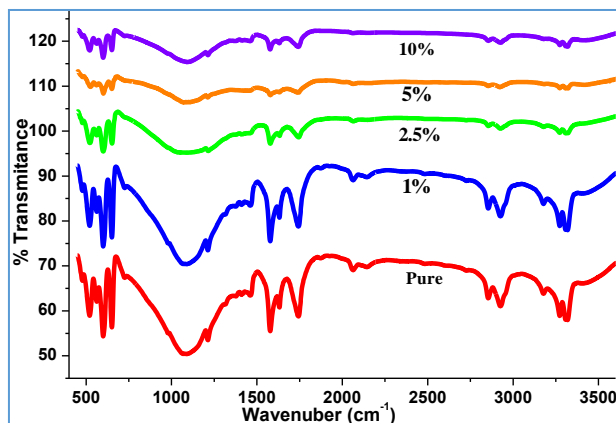


Fig. 2. FTIR spectra of pure and Mn doped CdS nanoparticles

3.3. XRD analysis

PXRD patterns of pure and Mn-doped CdS samples are shown in Fig. 4; analysis of undoped and Mn-doped CdS nanoparticles gave three prominent peaks at 2θ value of 26.76° , 29.92° and 34.32° angles corresponding to characteristic Bragg peaks of (111), (200) and (220) which corresponded to the cubic structure of CdS nanoparticles [19]. This showed that in the reaction pure cubic structure of CdS nanoparticles was formed. The intensities of the peaks observed were varying from the pure to Mn doped CdS nanoparticles which may be due to the replacement of Cd^{2+} by Mn^{2+} ions. The ionic radius of Mn is smaller than Cd which showed that lattice constant was decreased when CdS is doped with Mn. Hence a decrease in the sharpness of the diffraction peaks was observed in the Mn doped CdS. Average crystallite size was determined from the broadening of the first plane of the XRD pattern by using the Scherrer formula given in equation (1).

$$L = k\lambda/\beta_{1/2}\cos\theta \quad (1)$$

where θ is the Bragg's angle and λ is the wavelength (1.5418 \AA) of X-rays used (Cu source used), $\beta_{1/2}$ is full peak width at half maximum (FWHM) of the pure diffraction profile in radians on 2θ scale, and k is constant which is approximately equal to unity and related both to the crystal shape and to the way in which θ is defined [20]. In XRD pattern no change in the peak at 2θ positions was observed with doping of Mn in the CdS nanoparticles and hence the doping of Mn on the CdS nanoparticles did not affect the structure of CdS nanoparticles and showed cubic structure in all samples. The average crystallite size of the pure and Mn doped CdS nanoparticles were calculated using the Scherrer equation; the average crystallite size of CdS nanoparticles was thus found about $\sim 78 \pm 5 \text{ nm}$. The average crystallite size of 1%, 2.5%, 5% and 10% Mn doped CdS nanoparticles thus found were 70 nm, 65 nm, 55 nm and 45 nm respectively, ably supported by FE-SEM analysis too.

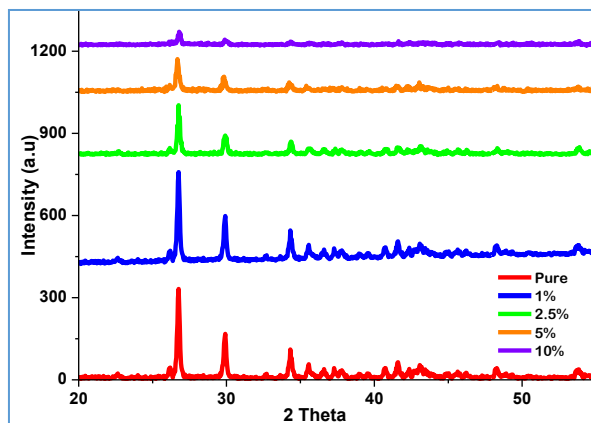


Fig. 4: XRD patterns of (a) Pure CdS nanoparticles (b) 1% Mn doped (c) 2.5% Mn doped (d) 5% Mn doped and (e) 10% Mn doped CdS nanoparticles

3.4. EDX Analysis

Fig.5 showed the elemental composition of the CdS nanoparticles with the help of energy dispersive X-ray (EDX). EDX spectra showed strong signals for Cd and S, proving the reduction of Cd^{2+} into CdS nanomaterials and the appearance of additional peaks was due to the presence of capping agents. As shown in the EDX spectra a clear signal for Mn was also present in the Mn-doped CdS nanoparticles [21]. The spectra contained strong peaks for oxygen which may be due to the presence of capping agents and due to CdO formation as the samples of nanoparticles were kept in ambient conditions so CdO formation is not surprising.

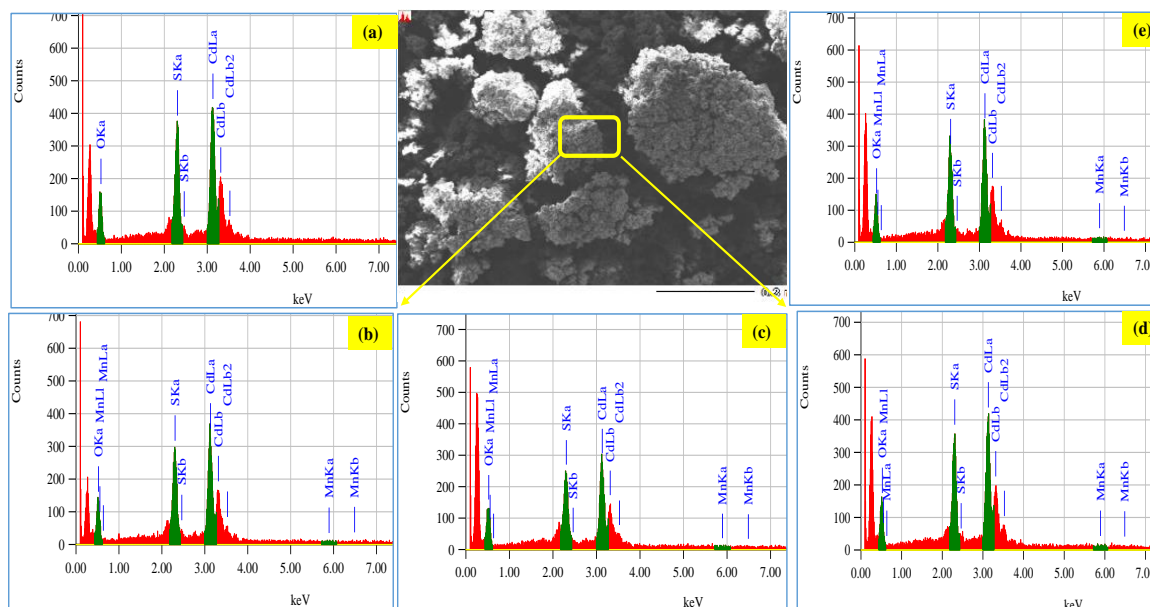


Fig. 5: EDX analysis of (a) Pure CdS nanoparticles (b) 1% Mn doped (c) 2.5% Mn doped (d) 5% Mn doped and (e) 10% Mn doped CdS nanoparticles

3.5. SEM Analysis

Morphology and size of pure and Mn-doped CdS nanoparticles were analyzed using SEM and shown in Fig. 6 and 7. It has been reported in the literature that the optical and electronic properties of nanoparticles depend on their shapes [22]; for surface morphology and size determination SEM has been used by several investigators previously for characterization of

nanoparticles [23]. The synthesized CdS nanoparticles were spherical in shape and polydispersed. The crystallite size thus obtained for CdS nanoparticles from SEM was found within the range of 62-100 nm (mean size of about $\sim 80 \pm 4$ nm) ably supported by XRD pattern too. While the average crystallite size of Mn doped CdS nanoparticles for 1%, 2.5%, 5% and 10% obtained from SEM was 73 nm, 68 nm, 59 nm and 50 nm respectively. The images ratified the formation of some nanoparticles capped with castor oil. This advocates that castor oil worked as surfactants which prevented the particle from the internal agglomeration, showing the stabilization of the nanomaterials[24].

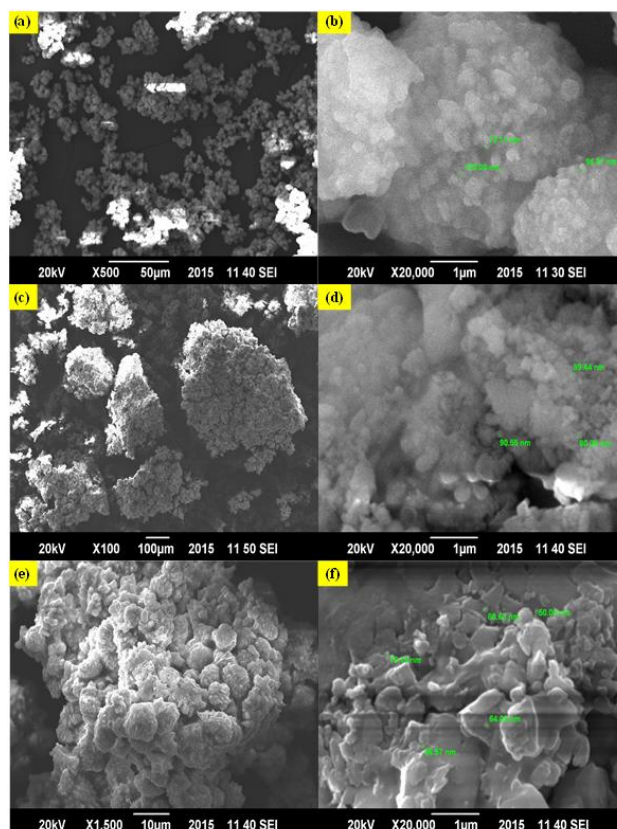


Fig. 6. Low and high magnification SEM micrographs of pure CdS (a,b), 1% Mn-doped CdS (c,d) and 2.5% Mn-doped CdS nanoparticles

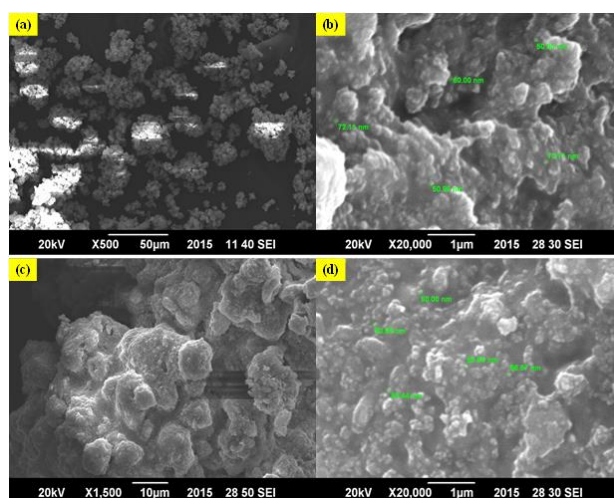


Fig. 7. (a & b) Low to high magnified SEM images of 5% Mn doped CdS and (e & f) Low to high magnified SEM images of 10% Mn doped CdS nanoparticles

3.6. Photoluminescence (PL) Study of pure and Mn-doped CdS NPs

Fig. 8 shows the normalized PL spectra for pure and Mn-doped CdS nanoparticles in the range of 300 to 700 nm at room temperature. Photoluminescence property of CdS nanoparticles is very sensitive to the size and surface defect. The possible defects in CdS nanoparticles are the vacancies of cadmium (V_{Cd}), vacancies of sulfur (V_s), cadmium interstitials (I_{Cd}^+) and sulfur interstitials (I_s) [25]. The PL spectrum of CdS nanoparticles showed emission peak at ~570 nm. However, Mn-doped CdS nanoparticles exhibited two major emission peaks, a broad emission peak around at ~590 nm and one small emission peak at ~646 nm. The green emission at ~590 nm may be due to radiative recombination of holes and electrons via the defect/surface states present in the nanoparticles [26, 27]. The decrease in PL intensity in the green emission of Mn doped CdS nanoparticles indicated the transfer of energy from excited carriers trapped at the surface to Mn^{2+} ions [28]. Maximum PL emission intensity was found for the concentration of 1 mol% Mn. PL emission intensity decreasing by increasing the Mn^{2+} concentration. It has been also reported in the literature that above 2-3 mol% Mn^{2+} concentrations the reduction in PL may occur due to Mn-Mn interactions [29].

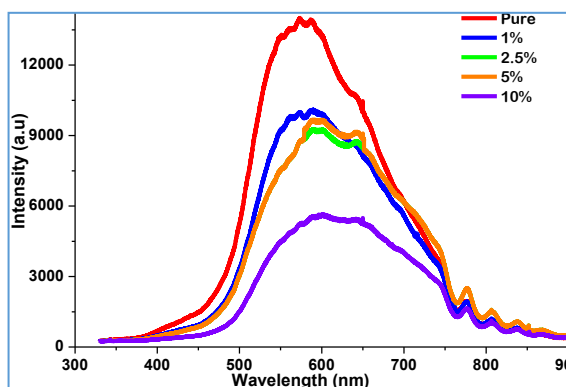


Fig. 8. PL spectra of pure and Mn-doped CdS nanoparticles synthesized by microwave assisted method.

4. Conclusions

In the present work, we have successfully developed a novel green synthesis method for the CdS nanoparticles via a microwave assisted methods using castor oil as capping agent and hydrazine as reducing agent in deionized water. CdS nanoparticles have been analyzed by UV-Vis, FTIR, XRD, EDX, SEM and PL and the increase in Mn concentration resulted in decrease in the size of the nanoparticles. The crystalline shape of the nanoparticles doesn't affect by increasing Mn concentrations. The decreases in PL of nanoparticles were observed with increase in Mn^{2+} concentration. The decrease in PL intensity of Mn doped CdS nanoparticles indicate the transfer of energy from excited carriers trapped at the surface to Mn^{2+} ions.

References

- [1] V. Nogrinya, J.K. Dongre, M. Ramrakhiani, B.P. Chandra, Chalcogenide Lett. **5**, 365 (2008).
- [2] S. Erra, C. Shivakumar, H. Zhao, K. Barri, D. Morel, C. Ferekides, Thin Solid Films **515**, 5833 (2007).
- [3] P. Bansal, N. Jaggi, S.K. Rohilla, Res. Chem. Sci. **2**, 69 (2012).
- [4] E.C.D.L.C. Terrazas, R.C.A.Lázaro, M.L.M.González, P.A. Luque, S.J. Castillo, A. Carrillo-Castillo, Chalcogenide Lett. **12**, 147 (2015)
- [5] S. Suresh, S.S.R.S. Anand, R. Arul, D. Isha, Chalcogenide Lett. **13**, 291 (2016).
- [6] K. R. Murali, C. Kannan, P. K. Subramanian, Chalcogenide Lett. **5**, 195 (2008).

- [7] M.F. Kotkata, A.E. Masoud, M.B. Mohamed, E.A. Mahmoud, *Chalcogenide Lett.* **5**, 209 (2008).
- [8] R. Demir, F. Gode, *Chalcogenide Lett.* **12**, 43 (2015).
- [9] N. Kumar, L.P. Purohit, Y.C. Goswami, *Chalcogenide Lett.* **12**, 333 (2015).
- [10] C. Jing, X. Xu, X. Zhang, Z. Liu, J. Chu, *J. Phys. D Appl. Phys.* **42**, 075402 (2009).
- [11] J.R. Lakowicz, I. Gryczynski, J. Piszczek, C.J. Murphy, *J. Phy. Chem. B* **106**, 5365 (2002).
- [12] W. Posthumus, P.C. Magusin, M.M. Broken-Zijp, J.C. Tinnemans, A.H. Van der, *J. Colloid and Interface Science*, **269**, 109 (2004).
- [13] A. Din, S.B. Khan, M.I. Khan, S.A.B. Asif, M.A. Khan, S. Gul, K. Akhtar, A.M. Asiri, *J. Mater. Sci. Mater. Electron.* **Accepted Article** (2016). DOI: 10.1007/s10854-016-5633-8
- [14] R.A. Devi, M. Latha, S. Velumani, G. Oza, P. Reyes-Figueroa, M. Rohini, I.G. Becerril-Juarez, I.G. Lee, J. Yi, *J. Nanosci. Nanotechnol.* **15** 843 (2015).
- [15] A. Lopez, A. Vazquez, I. Gomez, *Rovista Mexicana de Fisica* **59**, 160 (2013).
- [16] S. Gul, M. Ismail, M. I. Khan, S.B. Khan, A.M. Asiri, I.U. Rahman, M.A. Khan, M.A. Kamboh, *Asian Pac. J. Trop. Dis.* **6**(4), 311 (2016).
- [17] M.M. Rahman, S.B. Khan, G. Gruner, M.S. Al-Ghamdi, M.A. Daous, A.M. Asiri, *Electrochim. Acta* **103**, 143 (2013).
- [18] L. Yemei, M. An, G. Lu, *Appl. Surf. Sci.* **253**, 459 (2006).
- [19] H. Metin, R. Esen, *J. Cryst. Growth*, **258**, 141 (2004).
- [20] J. Lee, *Appl. Surf. Sci.* **252**, 1398 (2005).
- [21] S. Basavaraja, S. Balaji, A. Lagashetty, A. Rajasab, A. Venkataraman, *Mater. Res. Bulletin* **43**, 1164 (2008).
- [22] R.S. Yadav, R. Mishra, A.C. Pandey, *J. Exp. Nanosci.* **4**, 139 (2009).
- [23] J. Barman, J. P. Borah, K. C. Sarma, *Chalcogenide Lett.* **5**, 265 (2008).
- [24] R. Sankar, A. Karthik, A. Prabu, S. Karthik, K. S. Shivashangari, V. Ravikumar, *Colloids Surf. B.* **108**, 80 (2013).
- [25] S. K. Mishra, R. K. Srivastava, S. G. Prakash, R. S. Yadav, A.C. Panday. *J. Alloys Compd.* **513**, 118 (2012).
- [26] B. Zhou, Z. Liu, H. Wang, Y. Yang, W. Su, *Catal. Lett.* **132**, 75 (2009).
- [27] C. Wang, H.M. Wang, Z.Y. Fang, *J. Alloys Compd.* **486**, 702 (2009).
- [29] A. Nag, S. Sapra, S.S. Gupta, A. Prakash, A. Ghangrekar, N. Periasamy, D.D. Sharma, *Bull. Mater. Sci.* **31**, 561 (2008).
- [30] S. Taguchi, A. Ishizumi, T. Tayagaki, Y. Kanemitsu, *Appl. Phys. Lett.* **94**, 173101 (2009).